

Published in final edited form as:

Gene Expr Patterns. 2008 January ; 8(2): 124–139. doi:10.1016/j.modgep.2007.09.003.

Characterization of the mid-foregut transcriptome identifies genes regulated during lung bud induction

Guetchyn Millien¹, Jennifer Beane^{1,4}, Marc Lenburg³, Po-Nien Tsao¹, Jining Lu¹, Avrum Spira^{1,2,4}, and Maria I. Ramirez^{1,2,*}

¹ Pulmonary Center, Department of Medicine, Boston University School of Medicine, Boston, MA 02118

² Department of Pathology, and Laboratory Medicine, Boston University School of Medicine, Boston, MA 02118

³ Department of Genetics and Genomics, Boston University School of Medicine, Boston, MA 02118

⁴ Bioinformatics Program, Boston University College of Engineering, Boston, MA 02118

Abstract

To identify genes expressed during initiation of lung organogenesis, we generated transcriptional profiles of the prospective lung region of the mouse foregut (mid-foregut) microdissected from embryos at three developmental stages between embryonic day 8.5 (E8.5) and E9.5. This period spans from lung specification of foregut cells to the emergence of the primary lung buds. We identified a number of known and novel genes that are temporally regulated as the lung bud forms. Genes that regulate transcription, including DNA binding factors, co-factors, and chromatin remodeling genes, are the main functional groups that change during lung bud formation. Members of key developmental transcription and growth factor families, not previously described to participate in lung organogenesis, are expressed in the mid-foregut during lung bud induction. These studies also show early expression in the mid-foregut of genes that participate in later stages of lung development. This characterization of the mid-foregut transcriptome provides new insights into molecular events leading to lung organogenesis.

Keywords

Lung; development; organogenesis; foregut; endoderm; embryo; mouse; microarray; RNA amplification; gene expression; real time PCR; laser capture microdissection; transcription factors; chromatin remodeling; Fox; Notch

Between E7.5 and E9.5 of mouse development, remarkable morphogenetic changes take place in the ventral foregut resulting in formation of distinct organs including pancreas, liver, thyroid, and lung (Grapin-Botton and Melton, 2000; Wells and Melton, 1999). Organ-specific genes such as Pdx1 (pancreas) (Murtaugh and Melton, 2003), albumin (liver) (Jung et al., 1999), Hhex and Pax8 (thyroid) (Parlato et al., 2004) and thyroid transcription factor 1 (thyroid and lung) (DeFelice et al., 2003; Desai et al., 2004; Kimura et al., 1999) demarcate different regions

*Corresponding author. Boston University School of Medicine., Evans Biomedical Research Center, 650 Albany St., X-440, Boston, MA 02118., E-mail address: mramirez@bu.edu, Fax: +1-617-638-7530.

Publisher's Disclaimer: This is a PDF file of an unedited manuscript that has been accepted for publication. As a service to our customers we are providing this early version of the manuscript. The manuscript will undergo copyediting, typesetting, and review of the resulting proof before it is published in its final citable form. Please note that during the production process errors may be discovered which could affect the content, and all legal disclaimers that apply to the journal pertain.

of the foregut as development progresses. By E9 of development, embryos containing between 16 and 20 somites already show thyroid, liver and pancreas primordia but the mid-foregut region, between the pharyngeal arches and the liver and pancreas buds, is still a tube that shows no sign of lung bud formation. In this environment, the trachea and the lung evaginate from the ventral and ventrolateral foregut respectively at approximately E9.5 (Cardoso and Lu, 2006; Warburton et al., 2005). These developmental events are regulated by fibroblast growth factors, bone morphogenetic proteins, retinoic acid, and sonic hedgehog, and their receptors among other factors (Bellusci et al., 1997; Desai et al., 2004; Jung et al., 1999; Litingtung et al., 1998; Rossi et al., 2001; Sakiyama et al., 2003; Sekine et al., 1999; Warburton et al., 2005; Weaver et al., 2000). These signaling networks activate downstream effectors in both foregut mesoderm and endoderm to induce organ specific gene expression (Cleaver and Krieg, 2001; Horb, 2000; Jung et al., 1999; Kumar et al., 2003; Matsumoto et al., 2001; Wells and Melton, 2000).

Compared to the detailed understanding of the programs leading to formation of the liver and pancreas (Bort et al., 2006; Lee et al., 2005; Lemaigre and Zaret, 2004; Murtaugh and Melton, 2003; Serls et al., 2005; Tremblay and Zaret, 2005), the lung morphogenetic program has not been explored in detail, in large part due to the paucity of marker molecules known to be expressed in the presumptive lung region of the foregut. Microarray studies have been used to characterize profiles of gene expression in embryonic tissues including preimplantation mouse embryos (Sherwood et al., 2007; Zeng et al., 2004), pre-pancreas and early pancreatic endodermal cells (Gu et al., 2004). The latter database has been particularly important for the identification of genes involved in acquisition of pancreatic cell fate and has also established the transcriptional profiles of endodermal precursors. To date, global profiles of gene expression in the developing lung have been focused on the processes of branching morphogenesis and on perinatal lung development (Banerjee et al., 2004; Bonner et al., 2003; Lu et al., 2005; Lu et al., 2004a), but there are not yet similar data on molecular changes that accompany the initiation of lung organogenesis.

We report herein the characterization of the transcriptome of the lung region of the foregut (referred as mid-foregut) prior and during initiation of lung organogenesis, including trachea and primary bud formation. We have identified genes expressed in mid-foregut cells, and genes whose expression levels change during lung primordium formation.

1. RESULTS AND DISCUSSION

1.1 Developmental lung genes are expressed in the prospective lung region of the foregut

We studied temporal differences in gene expression in mid-foregut tissues containing endoderm and mesoderm cells isolated by microdissection at three developmental stages prior and after lung bud formation (16–20, 21–25 and 26–30 somite stages) (Figure 1A, B). We determined by real time RT-PCR (QRT-PCR) whether the tissues to be used in the microarray studies expressed lung and liver marker genes. Twenty four hours before lung budding, at E8.5, the mid-foregut already expresses lung developmental genes. Thyroid transcription factor 1 (Ttf-1, TTF-1, Nkx2.1), a transcription factor critical for lung cell differentiation (Kimura et al., 1999), was detected in the mid-foregut tissue at all three developmental stages, and the level of expression was increased as the primary lung buds formed (Figure 1C); although Ttf-1 is also expressed during thyroid organogenesis, the thyroid was excluded from the mid-foregut samples analyzed, as shown in Figure 1A–B. Fibroblast growth factor 10 (FGF10) expressed in the foregut mesenchyme can be detected at the three developmental stages, and significantly increases in 26–30 somite vs. 21–25 somite foreguts (Figure 1C). Surfactant protein C (SP-C) mRNA, a lung-specific gene (Khour et al., 1994; Wang et al., 1994), expressed very early in lung development and a downstream target of Ttf-1, was not detected in 16–20, 21–25 or 26–30 somite embryos by QRT-PCR (data not shown) but can be detected later in the mid-foregut

endoderm of embryos containing more than 30 somites (Figure S1A–B, supplementary material). Albumin mRNA was not detected in the mid-foregut by real time PCR (data not shown), but is highly detected in the posterior foregut endoderm (liver), isolated by laser capture microdissection from embryos containing more than 30 somites (Figure S1A–B, supplementary material). Microarray analyses of amplified mid-foregut RNA show expression of the lung expressed genes *T1a* and *caveolin-1* (Ramirez et al., 2002; Williams et al., 1996), and marked reduction of the liver genes α -fetoprotein and transthyretin (Jung et al., 1999; Lee et al., 2005), as development proceeds (Table S3, supplementary material). *Pax8*, a thyroid gene expressed also in the branchial arches (Trueba et al., 2005) was detected at low levels in the 16–20 somite samples, and its level remains low and unchanged during lung bud formation (Table S3, supplementary material). Overall, these data confirm the specific nature of the regions selected to study. The exact timing of lung cell specification in the multipotent foregut has not been clearly determined, but detection of *Titf-1* and *FGF10* in the mid-foregut at E8.5 indicates certain commitment of the cells to start lung formation (Desai et al., 2004).

1.2 Statistical analysis and functional classification of the microarray data

Three independent mRNA samples, at each of the developmental stages selected (16–20s, 21–25s, and 26–30s), were amplified and analyzed by microarrays (total of 9 arrays). Hierarchical clustering analysis of genes significantly up-regulated or down regulated across all nine samples, with ANOVA and Student's t-test $p \leq 0.05$ and detection $p \leq 0.05$ are shown in Figures 2A and 2B. The result illustrates that the general premise of this study is correct, i.e. that significant changes in gene expression accompany the induction of the lung as it emerges from the foregut at the 26–30 somite stage.

A number of comparisons are possible to analyze the data. We chose to identify differences between early and late foreguts as representing the absence and the presence of lung buds. Relative to the earliest group, 104 genes are up-regulated more than 1.8 fold and 119 genes down-regulated more than 1.8 fold in the late group undergoing lung organogenesis. Although a change higher than 2-fold has been conventionally used to consider genes as functionally important, we have opted to use 1.8 fold as cut-off level due to the high number of genes showing a statistically significant change between 1.8 and 2-fold. A number of previous studies also opted to use lower cut-off levels (1.2–1.5) when the changes are highly significant (Jeong et al., 2005; Lu et al., 2004b; McReynolds et al., 2005). Enriched biological themes within the up-regulated genes and the down-regulated genes were identified using appropriate computer algorithms (Figure 2C–D). The most significantly overrepresented, up-regulated biological process (Ease score= 3.35×10^{-3}) was regulation of transcription (Figure 2C). That group contains largely, but not solely, transcription factors; many have not been previously shown to be related to lung development. Some of these transcription factors were further analyzed by QRT-PCR and whole mount in situ hybridization. Within the down-regulated genes, macromolecule/protein biosynthesis was the most significantly overrepresented biological process (Ease score= 3.23×10^{-9}) (Figure 2D). Some transcriptional regulatory genes were also down-regulated. Genes categorized as functioning in proliferation, transport, and organization and biogenesis are represented in both the up- and down-regulated groups.

To find genes enriched in each of the three time points studied, especially in the intermediate time point (21–25 somite stage), a parametric ANOVA was performed. 1076 probe sets with a p-value less than 0.05 were selected for further analysis by K-means clustering (Figure 3). Five clusters (A–E) were generated in which genes decline from 16–20 to 21–25 somites or to 26–30 somites, increase from the 16–20 somite stage with a peak at 26–30 somites, or peak in the middle at the 21–25 stage, or increase from 21–25 to 26–30 somites. We listed in Table 1 genes that are enriched in each developmental time point identified by ANOVA and/or Student's t tests, and are involved in transcriptional regulation. These genes include factors

that bind directly to cis-elements in the DNA, co-factors, and genes that form chromatin modifying complexes. For a complete list of genes see Tables S4–S6 in supplementary material.

1.3 Real time RT-PCR confirmation of temporal changes in gene expression

Forty three genes shown to change level of expression during lung induction were analyzed by QRT-PCR using non-amplified mid-foregut RNA. mRNA levels in 26–30 somite samples normalized to GAPDH mRNA levels were expressed relative to the 16–20 somite samples set at a relative value of one. A similar semi-quantitative comparison of the same genes was done for the microarray data. As shown in Figure 4A–B and Figure S3A–B, 19 out of 43 genes tested showed statistically significant changes in expression by QRT-PCR correlating well to the microarray data, although the absolute fold-differences do not match precisely as would be expected due the different nature of the methods and the analysis of different samples. In addition, the trend in expression patterns of other 12 genes (e.g. *Cbfa2t1*, *Cbx4*, *Six1*) was confirmed by QRT-PCR, although the fold change observed by this method was not statistically significant ($p > 0.05$) (Table S7A). The remaining 12 genes tested did not match the microarray data (Table S7B).

1.4 Transcription factors and co-factors are developmentally regulated as the lung buds form

The largest change demonstrated by QRT-PCR analysis is in the LIM domain transcription factor *Isl1* (Thor et al., 1991). *Isl1* is necessary for proliferation and survival of cells in the foregut mesoderm and dorsal pancreatic mesenchyme, and is linked to cell fate decision in motor neurons (Pfaff et al., 1996), cardiac cells (Cai et al., 2003), and pancreatic islets (Ahlgren et al., 1997) but has not been previously implicated in lung development. *Isl1* null mice [*Isl1* (–/–)] are developmentally arrested soon after E9.5, show abnormal organization of the vascular endothelium, and severely abnormal heart development with reduction of the amount of atrial tissue. Expression of *FGF10*, *Bmp4* and *Bmp7* is highly downregulated in pharyngeal endoderm and splanchnic mesoderm in the absence of *Isl1* at E8.5–9.0, likely as a result of direct or indirect regulation of these growth factors by *Isl1* and/or viability of the foregut cells. A recent publication indicates a putative cis-element for *Isl1* in the *FGF10* promoter (Ohuchi et al., 2005). We now show that *Isl1* is transiently expressed in the early stages of lung morphogenesis and its expression is down regulated as the lung begins branching morphogenesis. Early lethality of the *Isl1* null mutation precludes to study the role of *Isl1* in lung budding.

Other transcription factors that directly bind to DNA validated by QRT-PCR include *HoxA4* (Packer et al., 2000), *NFIB* (Chaudhry et al., 1997), and *Foxf2* (Aitola et al., 2000). We have identified by microarrays expression in the mid-foregut region of other *Fox* genes that were not previously linked to the process of lung bud formation. Most of the *Fox* genes were detected at high levels and did not change over the time period studied. *Fox* transcription factors play important roles in development (Lee et al., 2005), and during induction of the endoderm derived organs (Carlsson and Mahlapuu, 2002). *Foxa2* and *Foxa1* are critical for initial steps in foregut tube closing and viability of endodermal cells (Ang and Rossant, 1994). They also regulate expression of several lung genes including surfactant protein genes (Costa et al., 2001). Other *Fox* factors, such as *Foxf1*, *Foxp1*, and *Foxb1*, are regulators of later events in lung development (Costa et al., 2001).

Changes in level of expression of the *Dach2* co-factor, that belongs to the *Eya/Six/Dach* transcriptional complex involved in cell fate decisions in other organs (Davis et al., 2001), was validated by QRT-PCR. Three members of these complexes, *sine-oculis 1* (*Six1*) and *-5* (*Six5*) and *Daschund 2* (*Dach2*) change their level of expression as the lung buds; *Six1* is down regulated, and *Six5* and *Dach 2* are up-regulated. *Eya/Six/Dach* complexes can switch between

gene activation and repression of gene expression depending on the members of the family that form these complexes.

Four additional genes showing a large increase in 26–30 somite samples compared to 16–20 somite samples in the microarray analysis were measured by QRT-PCR of non-amplified mRNA and confirmed the original findings (Figure S3A–B, supplementary material). The putative functions of these molecules are diverse and include the enzymes alpha-2,8-sialyltransferase 8A (Yoshida et al., 1995) and 3-oxoacid CoA transferase 1 (Ganapathi et al., 1987), the apoptosis-related gene caspase 7 (Lakhani et al., 2006), and syndecan 2 (David et al., 1993) among others.

1.5 Expression of selected transcription factor and signaling gene families during lung bud formation

We evaluated microarray data for expression of members of the Fox, Hox, Tbx, GATA transcription factor families (Table 2) and genes of selected signaling pathways that participate in lung development including FGFs, Bmps, Shh, Retinoic Acid, and Notch pathways (Table 3) (Cardoso, 1995; Cardoso and Lu, 2006; Warburton et al., 2005). We have detected Foxa1, Foxa2, Hox A4, A5, B4, B5, B8; Tbx 1, 2; GATA 5, 6; FGF7, FGF1, FGFR2 and IV; Bmp4, and BmpR1a; Notch1 and Dll3 mRNAs among others. QRT-PCR confirmed that HoxA4 and Foxf2 (Figure 4A–B) are significantly increased in 26–30 somite samples. We anticipated finding expression of FGF10 and Ttf-1 (Nkx2.1) but these factors were not detected in the microarray analysis, possibly because they are of very low abundance, are poorly amplified prior to hybridization, and/or the oligos on the microarray are 5' to the amplified message region as the amplification method is 3' bias (Table S1); however these mRNAs can be readily detected by QRT-PCR in non-amplified mid-foregut samples (Figure 1C). Microarray analysis of amplified or non-amplified samples can always produce false positive or negative results. Therefore, validation by other methods is necessary. In this study we have analyzed selected genes by QRT-PCR and whole mount in situ hybridization.

The representation of members of the Fox family is notable as shown in Table 2. Of the 26 Fox family members represented on the microarrays used in the study, 12 are present in the mid-foregut (detection $p \leq 0.05$). Foxa1 and Foxa2 display the highest detection levels. However, with the exception of Foxp1 (Shu et al., 2001), Foxm1 (Kim et al., 2005) and Foxf2 (Wang et al., 2003) as shown in Tables 1 and 2, mRNA expression levels of other Fox genes do not change significantly during initiation of the lung budding. Among the signaling pathways, it is notable the number of Notch pathway related genes present in the mid-foregut as the lung forms (24 present in the mid-foregut out of 114 probe sets, Table 3). Changes in Notch 1 (Taichman et al., 2002), Delta-like 3 (Ladi et al., 2005), and presenilin enhancer 2 (Francis et al., 2002) are statistically significant. As the Notch pathway has been shown to regulate early cell fate decisions in other tissues (Louvi and Artavanis-Tsakonas, 2006), its role in lung induction will entail further evaluation.

1.6 Chromatin remodeling and DNA methylation genes change their level of expression during initiation of lung organogenesis

Among several chromatin remodeling genes identified in Table 1, smarce1/BAF57 and Ing3 were confirmed to increase their level of expression significantly as the lung buds. Smarce1/BAF57 is one of the genes that form part of the ATP-dependent chromatin remodeling SWI/SNF complex (Chen and Archer, 2005; Domingos et al., 2002) which modify nucleosomes changing the accessibility of transcription factors to their binding sites on the DNA (Sudarsanam and Winston, 2000). Ing3 is a component of the NuA4 histone acetyltransferase (HAT) complex (Doyon et al., 2004). These proteins are generally linked to gene activation.

Some polycomb family genes (PcG) such as *Suz12*, *Cbx4*, and *Rnf2* (Ringrose and Paro, 2004) and the DNA methylation genes *Dnmt3a* and *Mbd2* (Li, 2002) linked to gene silencing are up-regulated in the mid-foregut region as the lung bud forms. Many of these genes are ubiquitously expressed but an increase in the level of expression during lung induction highlights the importance of chromatin remodeling and DNA methylation in lung organogenesis (Lee et al., 2006).

1.7 Anterior-posterior patterns of gene expression in the foregut endoderm

The presence of distinct molecular fields within the anterior-posterior axis of the foregut endoderm was shown by QRT-PCR analysis of laser capture microdissected foregut epithelium that is free of adjacent mesenchymal cells (Figure 5A). This procedure allows the collection of regional epithelial samples representing anterior, mid, and posterior areas of the foregut endoderm. In 21–25 somite samples the patterns of expression of three transcription factors differ along the anterior-posterior foregut axis (Figure 5B). *Irx5*, a member of the Iroquois homeobox gene family expressed in the E9.5–10.5 foregut (Cohen et al., 2000), is expressed at similar levels in the three regions. In contrast *Hlxb9* mRNA is highly expressed in the most posterior sample with low to marginally detectable levels in the mid and anterior samples. This is consistent with its essential role in specification of gut epithelial cells to a pancreatic fate (Li et al., 1999). *FoxO1*, a homeobox transcription factor shown to inhibit pancreas-specific genes (Kitamura et al., 2002), is expressed in a linear gradient opposite to that of *Hlxb9* with the highest levels anteriorly. In 26–30 somite samples, the patterns of expression of three genes identified in the microarray analysis, *Isl1*, *Dach2*, and *smarce1/BAF57*, also differ along the anterior-posterior foregut axis (Figure 5C). *Isl1* is detected in the mid- and posterior foregut endoderm at similar levels, but higher than in the anterior endoderm. *Dach2*, is higher in the mid-foregut endoderm than in neighboring regions, while *smarce1* is higher in the posterior region, although it is expressed in other regions of the foregut.

1.8 Patterns of expression of genes identified in the microarray analysis

To further validate the microarray data we analyzed by whole mount in situ hybridization the pattern of expression of a number of genes involved in regulation of transcription. The transcription factor *Isl1* is significantly up-regulated in the mid-foregut at the time of lung bud formation by microarray and QRT-PCR analyses. Whole mount in situ hybridization performed in 26–30 somite embryos (E9.5) (Figure 6A and 6B) showed expression of *Isl1* mRNA in primary lung-bud mesenchyme. Although at this stage *Isl1* is no longer expressed in cardiac cells, it can be detected in the sinus venosus (Figure 6A). Expression is also high in the stomach region (Figure 6B). *Isl1* is essential for motor neuron differentiation and normal development of the heart, pancreas, and splanchnic mesenchyme, but its importance in lung development is not known due to the early lethal phenotype of the *Isl1* null mutant mice (Ahlgren et al., 1997; Cai et al., 2003; Pfaff et al., 1996; Thaler et al., 2004). Assessment of *Isl1* expression by QRT-PCR in total lung at different developmental time points shows that *Isl1* expression is transient, since the mRNA level peaks on embryonic day E9.5 and decreases at E11.5 to that of E8.5 (Figure 6C). This is followed by a gradual decline during later development to levels that are about 10–15% of the peak value. *Isl1* continue to be detected in adult lung although the levels are lower than the ones observed during lung budding.

Expression of the forkhead transcription factor *FoxG1* was localized in the mesenchyme of the primary lung buds at E9.5 and in the lung mesenchyme at E11.5 (Figure 6D–E). *FoxG1* is involved in morphogenesis of the telencephalon by controlling proliferation and differentiation of precursor cells (Martynoga et al., 2005). It participates in different signaling pathways. *FoxG1* interferes with TGF β pathway by association with Smad-interacting proteins (Seoane et al., 2004); it also interacts with the delta/notch/hes pathway by combining with Hes homodimers to repress transcription (Yao et al., 2001).

Two genes involved in chromatin modification identified in the microarray analysis, *Carm1* and *Cbx4*, were barely detected by whole mount in situ hybridization in the primary buds at E9.5 (data not shown). Their expression, though, is highly increased by E11.5. *Carm1* is concentrated in mesenchymal cells at the tips of the lung branches (Figure 6F), while *Cbx4* is in the epithelium (Figure 6I). *Carm1* (Coactivator associated arginine methyltransferase) is a transcriptional activator that interacts with the p160 family of nuclear receptor-associated factors and methylates histone 3 at arginine 17. Methylation of arginines by *Carm1* occurs along with acetylation of histones to remodel chromatin and recruit RNA polymerase II (Teyssier et al., 2002). *Cbx4* (Chromobox homolog 4) is one of the five mouse Polycomb homologs that act as transcriptional repressors. *Cbx4* binds to chromatin preferentially to histone 3 trimethylated in lysine 9 (H3K9me3) (Bernstein et al., 2006) and promotes SUMOylation of transcriptional repressors such as the DNA methyltransferase *Dnmt3a* (Li et al., 2007). Three other transcription factors *Zfp26* (Chowdhury et al., 1988), *musculin* (Lu et al., 1999), and *Rfx5* (Yong et al., 2007) that are up-regulated in the mid-foregut during lung budding (Table 1) can also be detected by whole mount in situ hybridization at E9.5 in a very distinctive pattern. *Zfp26*, a zinc-finger transcription factor is detected in the sub-epithelial mesenchyme of the primary buds (Figure 6G). At E10.5 it is barely detected with some expression remaining at the tips of the forming branches (Figure 6H). *Musculin*, or *MyoR*, a repressor of muscle differentiation that competes with the myogenic factor *MyoD*, is expressed in the mid-region of the foregut, in particular in the esophagus, but it is not expressed in the primary lung buds (Figure 6J). Expression can be detected also in the branchial arches and the stomach. The branchial arches continue to be positive at E10.5 and the lung is negative (Figure 6K). In contrast *Rfx5* is expressed in mesenchymal cells of the branchial arches, primary lung buds and stomach in the sub-epithelial layer (Figure 6L). Expression of *Zbtb1*, *Ing3*, *Rbbp4* and *Smarca1* was detected in the mid-region of the foregut and/or whole embryos at E9.5 by whole mount in situ hybridization but they are ubiquitously expressed (data not shown).

1.9 Concluding Remarks

In this study we have characterized the transcriptome of the mid-region of the mouse foregut during the period between lung specification of foregut cells and appearance of the initial lung buds. We have identified a substantial number of genes present in the prospective lung region, and genes that change their level of expression as the lung bud forms. We selected, for further studies, those involved in regulation of transcription since they were overrepresented among the genes that change as the lung forms, and because these factors likely activate the developmental program that sustains lung formation. The information generated, therefore, expands the list of genes to study new and known pathways driving lung progenitor cell differentiation and lung morphogenesis.

2. EXPERIMENTAL PROCEDURES

2.1 Isolation of mid-foregut tissue

We selected based on morphological features, three developmental stages to study gene expression profiles of mid-foregut tissue, containing endoderm and mesoderm cells. The stages are: 16–20 somite embryos, 21–25 somite embryos and 25–30 somite embryos. The earliest samples (16–20 somites) show evidence of primitive thyroid and liver/pancreas budding which provide morphologic limits at the extremes of the mid-foregut field from which the lung is derived. All embryos with greater than 25 somites have initiated formation of bilateral lung buds. Although some variability is expected in the relationship between somite number and morphology, there is a high degree of uniformity within the range of number of somites used to group the earliest and latest samples for molecular analysis.

Pregnant CD-1 mice were purchased from Charles River with pregnancy timed by the presence of a vaginal plug at day E0.5 of gestation. Dams were sacrificed at 6–12 hour intervals between gestational days E8.5 and E10 to obtain embryos containing between 16 and 30 somites. After hysterotomy, embryos were placed in PBS at 4°C prior to dissection. Each embryo was examined by dissecting microscopy to determine its somite number. Embryos were divided into three groups according to somite number: 16–20, 21–25, and 26–30 somites. This grouping correlates well with morphological features described above: 16–20 somite embryos have thyroid and liver buds but lack lung buds; all 26–30 somite embryos have lung, thyroid, and liver buds. The 20–25 somite group includes a small number of embryos in which lung buds have just commenced to emerge but are difficult to visualize. To obtain mid-foregut tissue, the neural tube and heart were dissected away for the embryo to expose the foregut. The foregut tissue posterior to the pharyngeal arches and anterior to the liver was excised using tungsten needles. Collected tissues were placed immediately in RNeasy™ buffer (QIAGEN). Five to ten mid-foreguts were pooled for each of the three somite groups for RNA analysis.

For histological analysis embryos or isolated mid-foreguts were fixed in 4% freshly prepared paraformaldehyde in PBS, stored in fixative overnight at 4°C, and embedded in paraffin following standard processing with ethanol dehydration. For laser capture microdissection embryos were fixed in 70% alcohol overnight at 4°C, dehydrated and embedded in paraffin in RNase-free conditions (Goldsworthy et al., 1999). Paraffin blocks were examined in a dissecting microscope with fiberoptic lighting to determine the orientation of the embryo. Excess paraffin was trimmed away, and the embryo was then reembedded oriented in a supine position (ventral side up). Six micron transverse sections were prepared for further study.

2.2 RNA purification and amplification and microarray quality controls

Total RNA was isolated from dissected tissues using RNeasy™ micropurification kit (QIAGEN) according to the manufacturer's directions, followed by treatment on column with DNA-free™ DNase (Ambion). RNA concentrations were measured in 1 µl (1/10 of the sample) in a NanoDrop ND-1000 spectrophotometer (NanoDrop Technologies). RNA (100 ng) was amplified using the RiboAmp HS kit (Arcturus Engineering, Inc) as described by the manufacturer. RNA was labelled using biotinylated ribonucleotides during the second *in vitro* transcription step using ENZO kit (Affymetrix). After two rounds of amplification, 10–15 µg of amplified RNA (aRNA) were obtained. The quality of amplified RNA obtained from microdissected foreguts was evaluated by examining the size distribution of the aRNA and aRNA from E18.5 fetal lung, used as control, in an agarose gel stained with Sybr Gold (Molecular Probes). A similar size distribution of aRNA in the three samples, ranging from ~200bp to > 2kb is shown in (Figure S2A, supplementary material). Thus the handling and time required for isolation of the samples has not resulted in degraded RNA unsuitable for microarray hybridization. Acceptable correlation values (R^2) values indicating reproducibility of microarrays are shown in Figure S2B (technical replicates $R^2 = 0.973$) and Figure S2C (biological replicates $R^2 = 0.969$) in the supplemental material.

2.3 Microarray experiments

Gene expression profiles of 3 independent mRNA samples for each of the three somite number groups were determined using MOE430 A2.0 microarrays (Affymetrix), containing 22,690 probe sets. Genes represented on this array are available at http://www.affymetrix.com/products/arrays/specific/mouse430_2.affx. Each scanned image was evaluated for significant artifacts. Bacterial genes spiked into the hybridization mixture (bioB and bioC) were used as positive quality controls for hybridization procedures. Arrays showing similar quality control parameters (Table S1, supplementary material) were used for data analysis. Background and noise measurements were below 100 in all arrays. The average ratio of signals from mid-sequence and 3' probe sets for GAPDH and actin was consistent

within all arrays, indicating similar efficiency of the amplification step. This allows comparison of amplified genes between independent arrays. As expected these ratios were higher than in non-amplified samples due to the preferential amplification of the 3' end of the mRNA using polydT. Minimal degradation of the isolated mRNA could have occurred, even though strict RNase-free conditions were used in every step of the experiments to avoid this problem. Data from each array was scaled (target intensity of 100) to normalize the results for inter-array comparisons. Reproducibility of the amplification and hybridization experiments was determined by correlation analysis of the microarray data obtained in replicates of 26–30 somite foregut RNA, starting from the same RNA (technical replicates) or from RNA from different embryos (biological replicates).

2.4 Microarray data analyses

A single weighted mean expression level for each gene was derived using Microarray Suite (MAS) 5.0 software (Affymetrix). Using a one-sided Wilcoxon signed-rank test, the MAS 5.0 software generated a detection p-value for each gene indicating whether or not the transcript was reliably detected. An initial mild filter was applied to select genes with detection p-value less than 0.05 in at least one of the nine arrays. A total of 13,371 probe sets passed the filter and were used in further statistical analyses. A parametric ANOVA was performed to find genes differentially expressed between two or more of the groups. 1076 genes passed the ANOVA test at $p < 0.05$, a significantly larger number than expected by chance (650 genes would be expected by chance). 80% of the 1076 genes were indeed detected in more than 7 arrays of the 9 arrays analyzed. While a significant proportion of genes identified on statistical analysis may represent false positives, we limited our biological analysis to those whose fold changes were greater than 1.8 fold. In addition, a large number of biologically relevant genes were validated by other methods. We performed a K-means clustering analysis with the 1076 genes that passed the ANOVA test ($p \leq 0.05$), to determine groups of genes that have similar time course profiles of expression levels over the three time points studied. To make the different genes comparable to each other in the cluster groups, the average of each sample group was calculated and z-score-normalized so the mean of the averages is zero and the standard deviation is one. K-means clustering was performed in Spotfire DecisionSite arbitrarily setting the number of clusters (k) equal to five. This method allows the identification of genes enriched in each of the somite groups. A Student's t-test was also performed ($p \leq 0.05$) to compare the earliest vs. the latest time point (16–20 somites to 26–30 somites). We used EASE (Expression Analysis Systematic Explorer, <http://david.abcc.ncifcrf.gov/ease/ease.jsp>), and the GO functional classification database to discover enriched biological themes within the lists of genes which are increased or decreased (> 1.8 fold) as the lung bud forms (16–20 somite samples vs. 26–30 somite samples). We have opted to use 1.8 fold as cut-off level due to the high number of genes showing a statistically significant change between 1.8 and 2-fold. The genes used in the EASE analysis pass ANOVA ($p \leq 0.05$) and Student's t tests ($p \leq 0.05$). EASE analyzes a list of Affymetrix ID numbers of the genes under study (input list) and finds over-represented biological "themes" in the list of genes, compared to the total number of genes for each biological theme in the array. The significance of each category is determined by two statistical values that are used to sort the categories i.e. the standard Fisher exact probability, and a conservative EASE score that identifies robust categories. We considered categories with an EASE score ≤ 0.05 as over-represented.

2.5 Real Time RT-PCR

Selected genes identified as differentially expressed in the mid-foregut by microarray analysis were validated by real time RT-PCR (QRT-PCR) in non-amplified mid-foregut RNA samples. Total non-amplified RNA from embryonic mid-foreguts grouped as before was treated with DNA-free™ DNase (Ambion) and reversed transcribed (RT) (1 µg of RNA in 25 µl reaction

volume) using AMV reverse transcriptase (Promega). RT reactions, diluted appropriately to obtain a signal in fewer than 34 cycles, were analyzed by QRT-PCR in an ABI 7000 Sequence Detection System (Applied Biosystems). PrimerExpress software version 2.0 (Applied Biosystems) was used to design primers for SybrGreen reactions, while TaqMan primers and probes used were Assays-on-Demand (Applied Biosystems) (Table S2, supplementary material). Reactions were performed in 50 μ l using SybrGreen PCR master mix or TaqMan PCR universal master mix (Applied Biosystems). Optimal reaction conditions were determined for all primers and probes and dissociation curves were generated for primers used in SybrGreen reactions to confirm a single PCR amplification product. A calibration curve, generated with serial dilutions of reverse transcribed E18.5 total lung or E8.5 total embryo RNA (n=3), was used to determine the relative message concentration for each gene tested. Data were normalized to relative concentration of GAPDH mRNA amplified from the same RT reaction. Using equal amounts of total RNA from 16–20, 21–25 and 26–30 somite groups we established that the relative expression level of GAPDH is similar at all three time points (data not shown). GAPDH was therefore used to normalize gene expression in QRT-PCR experiments.

2.6 Whole mount in situ hybridization

Whole mount in situ hybridization was performed as described by Wilkinson (Xu, 1998) and modified by Desai et al (Desai et al., 2004). Anti-sense and sense probes were generated by RT-PCR using oligonucleotides containing adaptors for T3 or T7 promoters (see oligonucleotide sequences in Table S8, supplementary material). Purified PCR fragments were used as templates in the *in vitro* transcription reaction (Maxiscript kit, Ambion) to synthesize sense and antisense riboprobes labeled with digoxigenin (DIG). After hybridization and staining of the embryos with BMpurple (Boehringer Mannheim), some were dehydrated and embedded in paraffin. Transverse sections (10 μ m) were obtained as described above, and counterstained with Fast Red using standard methods.

2.7 Laser Capture Microdissection (LCM) of foregut endoderm

We isolated endoderm cells from the anterior (thyroid region), mid (lung region) and posterior (liver/pancreas region) foregut of 21–25 and 26–30 somite embryos by laser capture microdissection. Embryos were fixed, embedded, and oriented in a supine position as described above. Six micron transverse sections were placed on plain glass slides, dried for 30 min at 37°C and immediately deparaffinized and dehydrated in xylenes (2 \times 5 min), absolute ethanol (30 sec) and xylenes (2 \times 5 min). Slides were dried at room temperature for 10 min and placed in slide boxes containing Drierite to keep them dry while dissecting. Foregut endoderm was microdissected using a PixCell I laser capture microdissection system (Arcturus) with a laser spot size of 30 μ , pulse power 15 mW, pulse width 15.2 ms. Sections from two embryos were collected per CapSure LCM cap (Arcturus) and total RNA was purified as described above. RNA purified from 6–10 embryos was pooled for QRT-PCR and [³²P]RT-PCR analyses.

Supplementary Material

Refer to Web version on PubMed Central for supplementary material.

Acknowledgements

We thank Drs. Mary C. Williams, Jerome S. Brody, Wellington W. Cardoso, and YuXia Cao for thoughtful comments about the manuscript. Dr. Norman Gerry for his technical support in the microarray data analysis. This work was supported by NHLBI Program Project Grant HL47049, and Doris Duke Charitable Foundation Clinical Scientist Development Award (A.S.).

References

- Ahlgren U, Pfaff SL, Jessell TM, Edlund T, Edlund H. Independent requirement for ISL1 in formation of pancreatic mesenchyme and islet cells. *Nature* 1997;385:257–60. [PubMed: 9000074]
- Aitola M, Carlsson P, Mahlapuu M, Enerback S, Pelto-Huikko M. Forkhead transcription factor FoxF2 is expressed in mesodermal tissues involved in epithelio-mesenchymal interactions. *Dev Dyn* 2000;218:136–49. [PubMed: 10822266]
- Ang SL, Rossant J. HNF-3 beta is essential for node and notochord formation in mouse development. *Cell* 1994;78:561–74. [PubMed: 8069909]
- Banerjee SK, Young HW, Barczak A, Erle DJ, Blackburn MR. Abnormal alveolar development associated with elevated adenine nucleosides. *Am J Respir Cell Mol Biol* 2004;30:38–50. [PubMed: 12855405]
- Bellusci S, Furuta Y, Rush MG, Henderson R, Winnier G, Hogan BL. Involvement of Sonic hedgehog (Shh) in mouse embryonic lung growth and morphogenesis. *Development* 1997;124:53–63. [PubMed: 9006067]
- Bernstein E, Duncan EM, Masui O, Gil J, Heard E, Allis CD. Mouse polycomb proteins bind differentially to methylated histone H3 and RNA and are enriched in facultative heterochromatin. *Mol Cell Biol* 2006;26:2560–9. [PubMed: 16537902]
- Bonner AE, Lemon WJ, You M. Gene expression signatures identify novel regulatory pathways during murine lung development: implications for lung tumorigenesis. *J Med Genet* 2003;40:408–17. [PubMed: 12807961]
- Bort R, Signore M, Tremblay K, Martinez Barbera JP, Zaret KS. Hex homeobox gene controls the transition of the endoderm to a pseudostratified, cell emergent epithelium for liver bud development. *Dev Biol* 2006;290:44–56. [PubMed: 16364283]
- Cai CL, Liang X, Shi Y, Chu PH, Pfaff SL, Chen J, Evans S. Isl1 identifies a cardiac progenitor population that proliferates prior to differentiation and contributes a majority of cells to the heart. *Dev Cell* 2003;5:877–89. [PubMed: 14667410]
- Cardoso WV. Transcription factors and pattern formation in the developing lung. *Am J Physiol* 1995;269:L429–42. [PubMed: 7485515]
- Cardoso WV, Lu J. Regulation of early lung morphogenesis: questions, facts and controversies. *Development* 2006;133:1611–24. [PubMed: 16613830]
- Carlsson P, Mahlapuu M. Forkhead transcription factors: key players in development and metabolism. *Dev Biol* 2002;250:1–23. [PubMed: 12297093]
- Chaudhry AZ, Lyons GE, Gronostajski RM. Expression patterns of the four nuclear factor I genes during mouse embryogenesis indicate a potential role in development. *Dev Dyn* 1997;208:313–25. [PubMed: 9056636]
- Chen J, Archer TK. Regulating SWI/SNF subunit levels via protein-protein interactions and proteasomal degradation: BAF155 and BAF170 limit expression of BAF57. *Mol Cell Biol* 2005;25:9016–27. [PubMed: 16199878]
- Chowdhury K, Rohdewold H, Gruss P. Specific and ubiquitous expression of different Zn finger protein genes in the mouse. *Nucleic Acids Res* 1988;16:9995–10011. [PubMed: 3143103]
- Cleaver O, Krieg PA. Notochord patterning of the endoderm. *Dev Biol* 2001;234:1–12. [PubMed: 11356015]
- Cohen DR, Cheng CW, Cheng SH, Hui CC. Expression of two novel mouse Iroquois homeobox genes during neurogenesis. *Mech Dev* 2000;91:317–21. [PubMed: 10704856]
- Costa RH, Kalinichenko VV, Lim L. Transcription factors in mouse lung development and function. *Am J Physiol Lung Cell Mol Physiol* 2001;280:L823–38. [PubMed: 11290504]
- David G, Bai XM, Van der Schueren B, Marynen P, Cassiman JJ, Van den Berghe H. Spatial and temporal changes in the expression of fibroglycan (syndecan-2) during mouse embryonic development. *Development* 1993;119:841–54. [PubMed: 8187643]
- Davis RJ, Shen W, Sandler YI, Heanue TA, Mardon G. Characterization of mouse Dach2, a homologue of *Drosophila* dachshund. *Mech Dev* 2001;102:169–79. [PubMed: 11287190]

- DeFelice M, Silberschmidt D, DiLauro R, Xu Y, Wert SE, Weaver TE, Bachurski CJ, Clark JC, Whitsett JA. TTF-1 phosphorylation is required for peripheral lung morphogenesis, perinatal survival, and tissue-specific gene expression. *J Biol Chem* 2003;278:35574–83. [PubMed: 12829717]
- Desai TJ, Malpel S, Flentke GR, Smith SM, Cardoso WV. Retinoic acid selectively regulates Fgf10 expression and maintains cell identity in the prospective lung field of the developing foregut. *Dev Biol* 2004;273:402–15. [PubMed: 15328022]
- Domingos PM, Obukhanych TV, Altmann CR, Hemmati-Brivanlou A. Cloning and developmental expression of Baf57 in *Xenopus laevis*. *Mech Dev* 2002;116:177–81. [PubMed: 12128220]
- Doyon Y, Selleck W, Lane WS, Tan S, Cote J. Structural and functional conservation of the NuA4 histone acetyltransferase complex from yeast to humans. *Mol Cell Biol* 2004;24:1884–96. [PubMed: 14966270]
- Francis R, McGrath G, Zhang J, Ruddy DA, Sym M, Apfeld J, Nicoll M, Maxwell M, Hai B, Ellis MC, Parks AL, Xu W, Li J, Gurney M, Myers RL, Himes CS, Hiebsch R, Ruble C, Nye JS, Curtis D. *aph-1* and *pen-2* are required for Notch pathway signaling, gamma-secretase cleavage of betaAPP, and presenilin protein accumulation. *Dev Cell* 2002;3:85–97. [PubMed: 12110170]
- Ganapathi MK, Kwon M, Haney PM, McTiernan C, Javed AA, Pepin RA, Samols D, Patel MS. Cloning of rat brain succinyl-CoA:3-oxoacid CoA-transferase cDNA. Regulation of the mRNA in different rat tissues and during brain development. *Biochem J* 1987;248:853–7. [PubMed: 2893604]
- Goldsworthy SM, Stockton PS, Trempus CS, Foley JF, Maronpot RR. Effects of fixation on RNA extraction and amplification from laser capture microdissected tissue. *Mol Carcinog* 1999;25:86–91. [PubMed: 10365909]
- Grapin-Botton A, Melton DA. Endoderm development: from patterning to organogenesis. *Trends Genet* 2000;16:124–30. [PubMed: 10689353]
- Gu G, Wells JM, Dombkowski D, Preffer F, Aronow B, Melton DA. Global expression analysis of gene regulatory pathways during endocrine pancreatic development. *Development* 2004;131:165–79. [PubMed: 14660441]
- Horb ME. Patterning the endoderm: the importance of neighbours. *Bioessays* 2000;22:599–602. [PubMed: 10878572]
- Jeong JW, Lee KY, Kwak I, White LD, Hilsenbeck SG, Lydon JP, DeMayo FJ. Identification of murine uterine genes regulated in a ligand-dependent manner by the progesterone receptor. *Endocrinology* 2005;146:3490–505. [PubMed: 15845616]
- Jung J, Zheng M, Goldfarb M, Zaret KS. Initiation of mammalian liver development from endoderm by fibroblast growth factors. *Science* 1999;284:1998–2003. [PubMed: 10373120]
- Khoor A, Stahlman MT, Gray ME, Whitsett JA. Temporal-spatial distribution of SP-B and SP-C proteins and mRNAs in developing respiratory epithelium of human lung. *J Histochem Cytochem* 1994;42:1187–99. [PubMed: 8064126]
- Kim IM, Ramakrishna S, Gusarova GA, Yoder HM, Costa RH, Kalinichenko VV. The forkhead box m1 transcription factor is essential for embryonic development of pulmonary vasculature. *J Biol Chem* 2005;280:22278–86. [PubMed: 15817462]
- Kimura S, Ward JM, Mino P. Thyroid-specific enhancer-binding protein/thyroid transcription factor 1 is not required for the initial specification of the thyroid and lung primordia. *Biochimie* 1999;81:321–7. [PubMed: 10401665]
- Kitamura T, Nakae J, Kitamura Y, Kido Y, Biggs WH 3rd, Wright CV, White MF, Arden KC, Accili D. The forkhead transcription factor Foxo1 links insulin signaling to Pdx1 regulation of pancreatic beta cell growth. *J Clin Invest* 2002;110:1839–47. [PubMed: 12488434]
- Kumar M, Jordan N, Melton D, Grapin-Botton A. Signals from lateral plate mesoderm instruct endoderm toward a pancreatic fate. *Dev Biol* 2003;259:109–22. [PubMed: 12812792]
- Ladi E, Nichols JT, Ge W, Miyamoto A, Yao C, Yang LT, Boulter J, Sun YE, Kintner C, Weinmaster G. The divergent DSL ligand Dll3 does not activate Notch signaling but cell autonomously attenuates signaling induced by other DSL ligands. *J Cell Biol* 2005;170:983–92. [PubMed: 16144902]
- Lakhani SA, Masud A, Kuida K, Porter GA Jr, Booth CJ, Mehal WZ, Inayat I, Flavell RA. Caspases 3 and 7: key mediators of mitochondrial events of apoptosis. *Science* 2006;311:847–51. [PubMed: 16469926]

- Lee CS, Friedman JR, Fulmer JT, Kaestner KH. The initiation of liver development is dependent on Foxa transcription factors. *Nature* 2005;435:944–7. [PubMed: 15959514]
- Lee TI, Jenner RG, Boyer LA, Guenther MG, Levine SS, Kumar RM, Chevalier B, Johnstone SE, Cole MF, Isono K, Koseki H, Fuchikami T, Abe K, Murray HL, Zucker JP, Yuan B, Bell GW, Herbolsheimer E, Hannett NM, Sun K, Odom DT, Otte AP, Volkert TL, Bartel DP, Melton DA, Gifford DK, Jaenisch R, Young RA. Control of developmental regulators by Polycomb in human embryonic stem cells. *Cell* 2006;125:301–13. [PubMed: 16630818]
- Lemaigre F, Zaret KS. Liver development update: new embryo models, cell lineage control, and morphogenesis. *Curr Opin Genet Dev* 2004;14:582–90. [PubMed: 15380251]
- Li B, Zhou J, Liu P, Hu J, Jin H, Shimono Y, Takahashi M, Xu G. Polycomb protein Cbx4 promotes SUMO modification of de novo DNA methyltransferase Dnmt3a. *Biochem J* 2007;405:369–78. [PubMed: 17439403]
- Li E. Chromatin modification and epigenetic reprogramming in mammalian development. *Nat Rev Genet* 2002;3:662–73. [PubMed: 12209141]
- Li H, Arber S, Jessell TM, Edlund H. Selective agenesis of the dorsal pancreas in mice lacking homeobox gene Hlx9. *Nat Genet* 1999;23:67–70. [PubMed: 10471501]
- Litingtung Y, Lei L, Westphal H, Chiang C. Sonic hedgehog is essential to foregut development. *Nat Genet* 1998;20:58–61. [PubMed: 9731532]
- Louvi A, Artavanis-Tsakonas S. Notch signalling in vertebrate neural development. *Nat Rev Neurosci* 2006;7:93–102. [PubMed: 16429119]
- Lu J, Izvolsky KI, Qian J, Cardoso WV. Identification of FGF10 targets in the embryonic lung epithelium during bud morphogenesis. *J Biol Chem* 2005;280:4834–41. [PubMed: 15556938]
- Lu J, Qian J, Izvolsky KI, Cardoso WV. Global analysis of genes differentially expressed in branching and non-branching regions of the mouse embryonic lung. *Dev Biol* 2004a;273:418–35. [PubMed: 15328023]
- Lu J, Webb R, Richardson JA, Olson EN. MyoR: a muscle-restricted basic helix-loop-helix transcription factor that antagonizes the actions of MyoD. *Proc Natl Acad Sci U S A* 1999;96:552–7. [PubMed: 9892671]
- Lu T, Pan Y, Kao SY, Li C, Kohane I, Chan J, Yankner BA. Gene regulation and DNA damage in the ageing human brain. *Nature* 2004b;429:883–91. [PubMed: 15190254]
- Martynoga B, Morrison H, Price DJ, Mason JO. Foxg1 is required for specification of ventral telencephalon and region-specific regulation of dorsal telencephalic precursor proliferation and apoptosis. *Dev Biol* 2005;283:113–27. [PubMed: 15893304]
- Matsumoto K, Yoshitomi H, Rossant J, Zaret KS. Liver organogenesis promoted by endothelial cells prior to vascular function. *Science* 2001;294:559–63. [PubMed: 11577199]
- McReynolds MR, Taylor-Garcia KM, Greer KA, Hoying JB, Brooks HL. Renal medullary gene expression in aquaporin-1 null mice. *Am J Physiol Renal Physiol* 2005;288:F315–21. [PubMed: 15507545]
- Murtaugh LC, Melton DA. Genes, signals, and lineages in pancreas development. *Annu Rev Cell Dev Biol* 2003;19:71–89. [PubMed: 14570564]
- Ohuchi H, Yasue A, Ono K, Sasaoka S, Tomonari S, Takagi A, Itakura M, Moriyama K, Noji S, Nohno T. Identification of cis-element regulating expression of the mouse Fgf10 gene during inner ear development. *Dev Dyn* 2005;233:177–87. [PubMed: 15765517]
- Packer AI, Mailutha KG, Ambrozewicz LA, Wolgemuth DJ. Regulation of the Hoxa4 and Hoxa5 genes in the embryonic mouse lung by retinoic acid and TGFbeta1: implications for lung development and patterning. *Dev Dyn* 2000;217:62–74. [PubMed: 10679930]
- Parlato R, Rosica A, Rodriguez-Mallon A, Affuso A, Postiglione MP, Arra C, Mansouri A, Kimura S, Di Lauro R, De Felice M. An integrated regulatory network controlling survival and migration in thyroid organogenesis. *Dev Biol* 2004;276:464–75. [PubMed: 15581879]
- Pfaff SL, Mendelsohn M, Stewart CL, Edlund T, Jessell TM. Requirement for LIM homeobox gene Isl1 in motor neuron generation reveals a motor neuron-dependent step in interneuron differentiation. *Cell* 1996;84:309–20. [PubMed: 8565076]

- Ramirez MI, Pollack L, Millien G, Cao YX, Hinds A, Williams MC. The alpha-isoform of caveolin-1 is a marker of vasculogenesis in early lung development. *J Histochem Cytochem* 2002;50:33–42. [PubMed: 11748292]
- Ringrose L, Paro R. Epigenetic regulation of cellular memory by the Polycomb and Trithorax group proteins. *Annu Rev Genet* 2004;38:413–43. [PubMed: 15568982]
- Rossi JM, Dunn NR, Hogan BL, Zaret KS. Distinct mesodermal signals, including BMPs from the septum transversum mesenchyme, are required in combination for hepatogenesis from the endoderm. *Genes Dev* 2001;15:1998–2009. [PubMed: 11485993]
- Sakiyama J, Yamagishi A, Kuroiwa A. Tbx4-Fgf10 system controls lung bud formation during chicken embryonic development. *Development* 2003;130:1225–34. [PubMed: 12588840]
- Sekine K, Ohuchi H, Fujiwara M, Yamasaki M, Yoshizawa T, Sato T, Yagishita N, Matsui D, Koga Y, Itoh N, Kato S. Fgf10 is essential for limb and lung formation. *Nat Genet* 1999;21:138–41. [PubMed: 9916808]
- Seoane J, Le HV, Shen L, Anderson SA, Massague J. Integration of Smad and forkhead pathways in the control of neuroepithelial and glioblastoma cell proliferation. *Cell* 2004;117:211–23. [PubMed: 15084259]
- Serls AE, Doherty S, Parvatiyar P, Wells JM, Deutsch GH. Different thresholds of fibroblast growth factors pattern the ventral foregut into liver and lung. *Development* 2005;132:35–47. [PubMed: 15576401]
- Sherwood RI, Jitianu C, Cleaver O, Shaywitz DA, Lamenzo JO, Chen AE, Golub TR, Melton DA. Prospective isolation and global gene expression analysis of definitive and visceral endoderm. *Dev Biol* 2007;304:541–55. [PubMed: 17328885]
- Shu W, Yang H, Zhang L, Lu MM, Morrisey EE. Characterization of a new subfamily of winged-helix/forkhead (Fox) genes that are expressed in the lung and act as transcriptional repressors. *J Biol Chem* 2001;276:27488–97. [PubMed: 11358962]
- Sudarsanam P, Winston F. The Swi/Snf family nucleosome-remodeling complexes and transcriptional control. *Trends Genet* 2000;16:345–51. [PubMed: 10904263]
- Taichman DB, Loomes KM, Schachtner SK, Guttentag S, Vu C, Williams P, Oakey RJ, Baldwin HS. Notch1 and Jagged1 expression by the developing pulmonary vasculature. *Dev Dyn* 2002;225:166–75. [PubMed: 12242716]
- Teyssier C, Chen D, Stallcup MR. Requirement for multiple domains of the protein arginine methyltransferase CARM1 in its transcriptional coactivator function. *J Biol Chem* 2002;277:46066–72. [PubMed: 12351636]
- Thaler JP, Koo SJ, Kania A, Lettieri K, Andrews S, Cox C, Jessell TM, Pfaff SL. A postmitotic role for Isl-class LIM homeodomain proteins in the assignment of visceral spinal motor neuron identity. *Neuron* 2004;41:337–50. [PubMed: 14766174]
- Thor S, Ericson J, Brannstrom T, Edlund T. The homeodomain LIM protein Isl-1 is expressed in subsets of neurons and endocrine cells in the adult rat. *Neuron* 1991;7:881–9. [PubMed: 1764243]
- Tremblay KD, Zaret KS. Distinct populations of endoderm cells converge to generate the embryonic liver bud and ventral foregut tissues. *Dev Biol* 2005;280:87–99. [PubMed: 15766750]
- Trueba SS, Auge J, Mattei G, Etchevers H, Martinovic J, Czernichow P, Vekemans M, Polak M, Attie-Bitach T. PAX8, TITF1, and FOXE1 gene expression patterns during human development: new insights into human thyroid development and thyroid dysgenesis-associated malformations. *J Clin Endocrinol Metab* 2005;90:455–62. [PubMed: 15494458]
- Wang J, Souza P, Kuliszewski M, Tanswell AK, Post M. Expression of surfactant proteins in embryonic rat lung. *Am J Respir Cell Mol Biol* 1994;10:222–9. [PubMed: 7509164]
- Wang T, Tamakoshi T, Uezato T, Shu F, Kanzaki-Kato N, Fu Y, Koseki H, Yoshida N, Sugiyama T, Miura N. Forkhead transcription factor Foxf2 (LUN)-deficient mice exhibit abnormal development of secondary palate. *Dev Biol* 2003;259:83–94. [PubMed: 12812790]
- Warburton D, Bellusci S, De Langhe S, Del Moral PM, Fleury V, Mailleux A, Tefft D, Unbekandt M, Wang K, Shi W. Molecular mechanisms of early lung specification and branching morphogenesis. *Pediatr Res* 2005;57:26R–37R.
- Weaver M, Dunn NR, Hogan BL. Bmp4 and Fgf10 play opposing roles during lung bud morphogenesis. *Development* 2000;127:2695–704. [PubMed: 10821767]

- Wells JM, Melton DA. Vertebrate endoderm development. *Annu Rev Cell Dev Biol* 1999;15:393–410. [PubMed: 10611967]
- Wells JM, Melton DA. Early mouse endoderm is patterned by soluble factors from adjacent germ layers. *Development* 2000;127:1563–72. [PubMed: 10725233]
- Williams MC, Cao Y, Hinds A, Rishi AK, Wetterwald A. T1 alpha protein is developmentally regulated and expressed by alveolar type I cells, choroid plexus, and ciliary epithelia of adult rats. *Am J Respir Cell Mol Biol* 1996;14:577–85. [PubMed: 8652186]
- Xu, Q.; Wilkinson, DG. *In situ hybridization: A practical approach*. Oxford University Press; London: 1998. p. 087-106.
- Yao J, Lai E, Stifani S. The winged-helix protein brain factor 1 interacts with groucho and hes proteins to repress transcription. *Mol Cell Biol* 2001;21:1962–72. [PubMed: 11238932]
- Yong X, Farmer SR, Smith BD. PPARgamma interacts with CIITA/RFX5 complex to repress collagen type I gene expression. *J Biol Chem*. 2007
- Yoshida Y, Kojima N, Tsuji S. Molecular cloning and characterization of a third type of N-glycan alpha 2,8-sialyltransferase from mouse lung. *J Biochem (Tokyo)* 1995;118:658–64. [PubMed: 8690732]
- Zeng F, Baldwin DA, Schultz RM. Transcript profiling during preimplantation mouse development. *Dev Biol* 2004;272:483–96. [PubMed: 15282163]

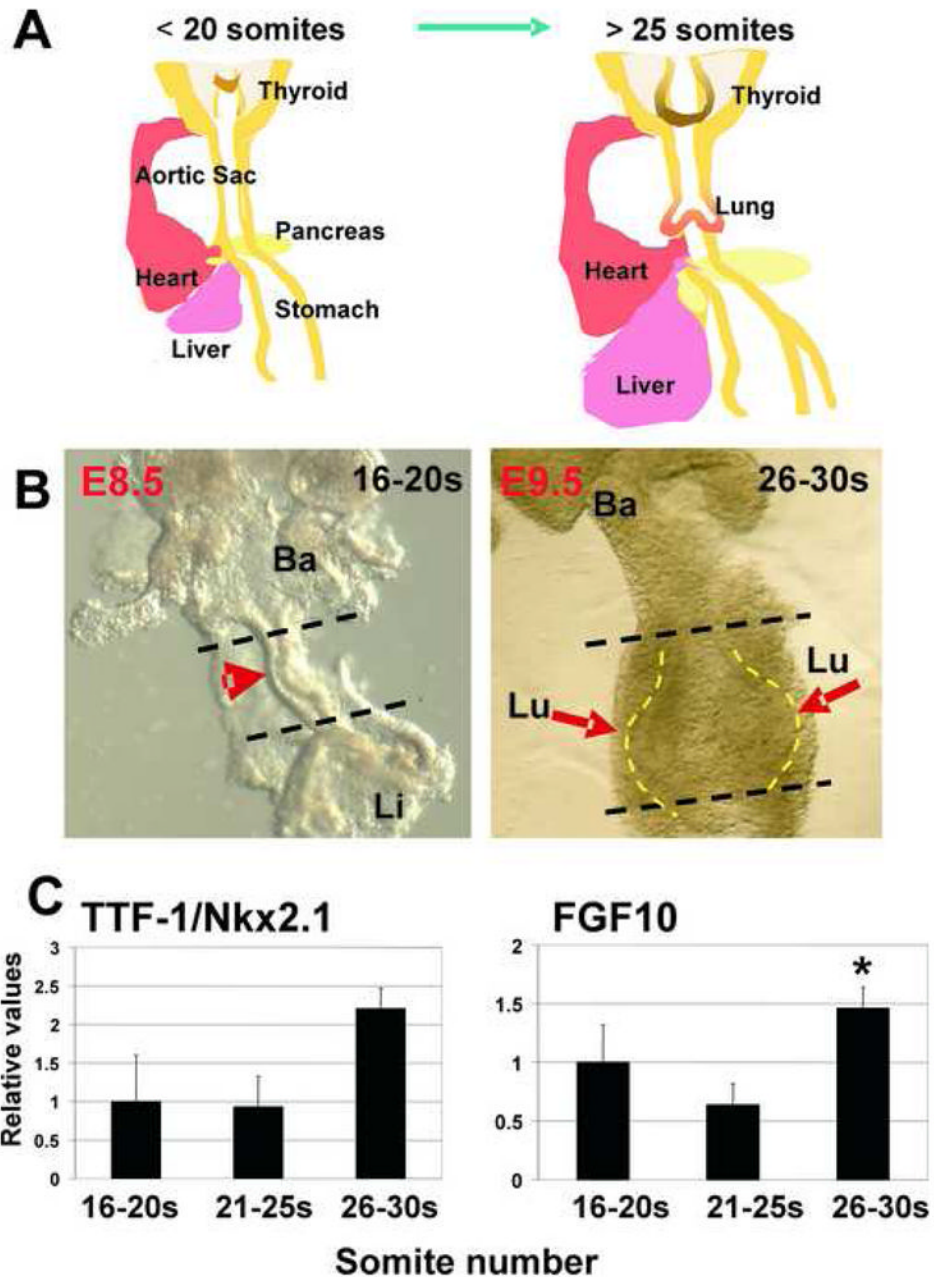


Figure 1. Mid-foregut tissue was isolated to study gene expression profiles at three developmental stages

A. Graphic representation of the morphology of the foregut in embryos containing 11–25 somites (E8.0–E9.5), and in embryos containing more than 25 somites (E9.5–10). Endoderm derived organs (thyroid, pancreas, liver, and lung) are depicted. The relative position of those organs to the cardiac mesoderm is represented. **B.** Microscopic appearances of partially dissected mid-foreguts from 16–20 somite embryos (E8.5) (red arrowhead), and from 26–30 somite embryos (E9.5). The mid-foregut tissue between the black dashed lines was collected for further analyses. The earliest samples (16–20 somites) show evidence of primitive thyroid and liver/pancreas budding at the extremes of the mid-foregut field from which the lung is derived. Embryos with greater than 25 somites have initiated formation of bilateral lung buds

(outlined in yellow). Ba, branchial arches; Li, liver; Lu, lung buds, outlined by yellow dashed lines. **C.** TTF-1 (Nkx2.1, Ttf1) and FGF10 mRNA levels, assessed by real time RT-PCR, in mid-foreguts dissected from 16–20, 21–25 and 26–30 somite mid-foreguts. Ttf-1 and FGF10 mRNA levels are normalized to GAPDH. Data are expressed relative to 16–20 somite mid-foregut samples. n=3 Error bars represent standard error of the mean. * indicates t-test ≤ 0.05 .

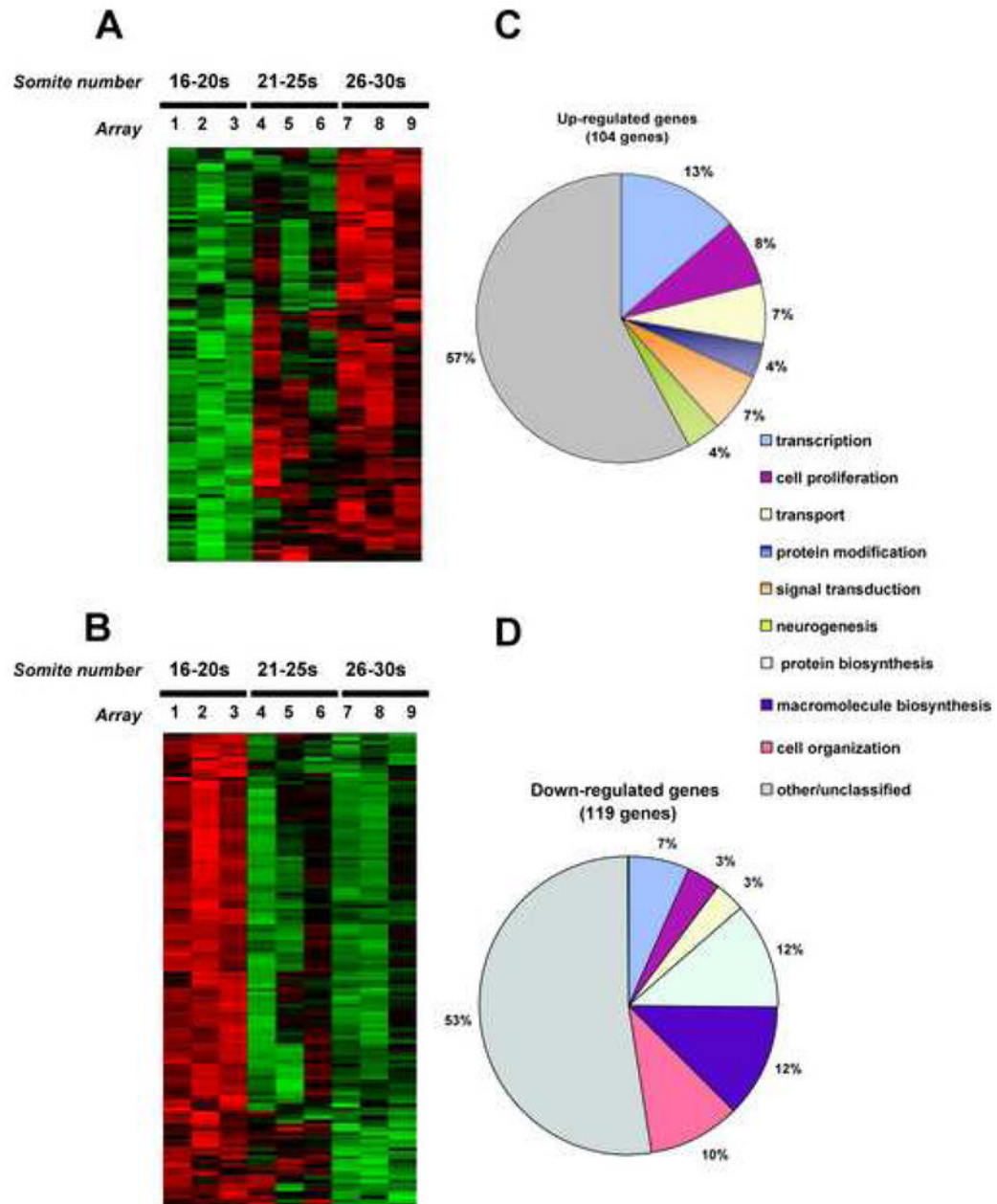


Figure 2.

Cluster graphs of **(A)** genes up-regulated ≥ 1.8 fold, and **(B)** genes down regulated ≥ -1.8 fold from 16–20 somite to 26–30 somite embryos (detection $p \leq 0.05$, ANOVA $p \leq 0.05$, and Student's test $p \leq 0.05$). Green color indicates low expression, red indicates high expression. Three independent arrays were analyzed for each developmental stage (arrays 1–3, 16–20 somite mid-foregut samples; arrays 4–6, 21–25 somite mid-foregut samples; arrays 7–9, 26–30 somite mid-foregut samples). **C.** Pie chart showing the GO classification of the functional groups of the 104 genes up-regulated shown in **A**. **D.** Pie chart showing the GO classification of the functional groups of the 119 genes down-regulated shown in **B**.

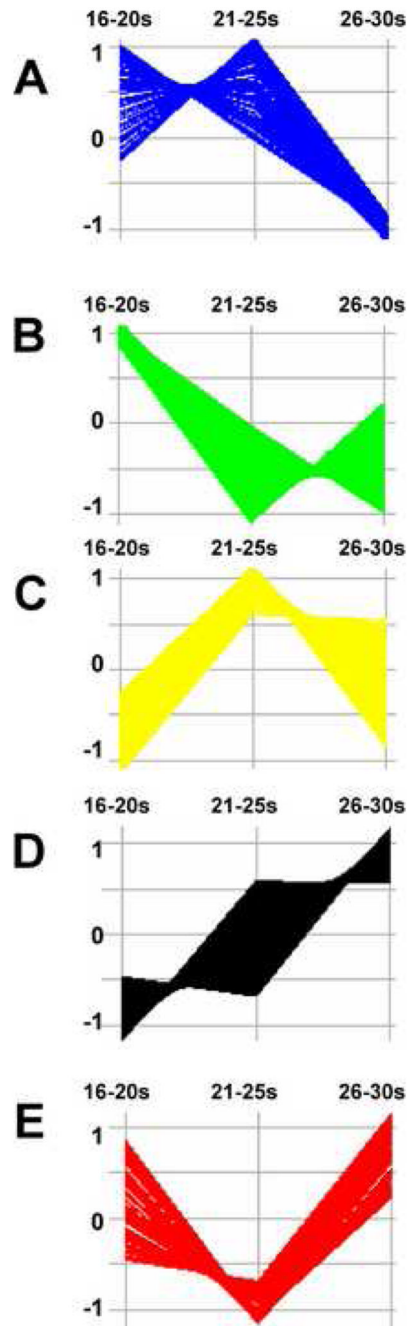
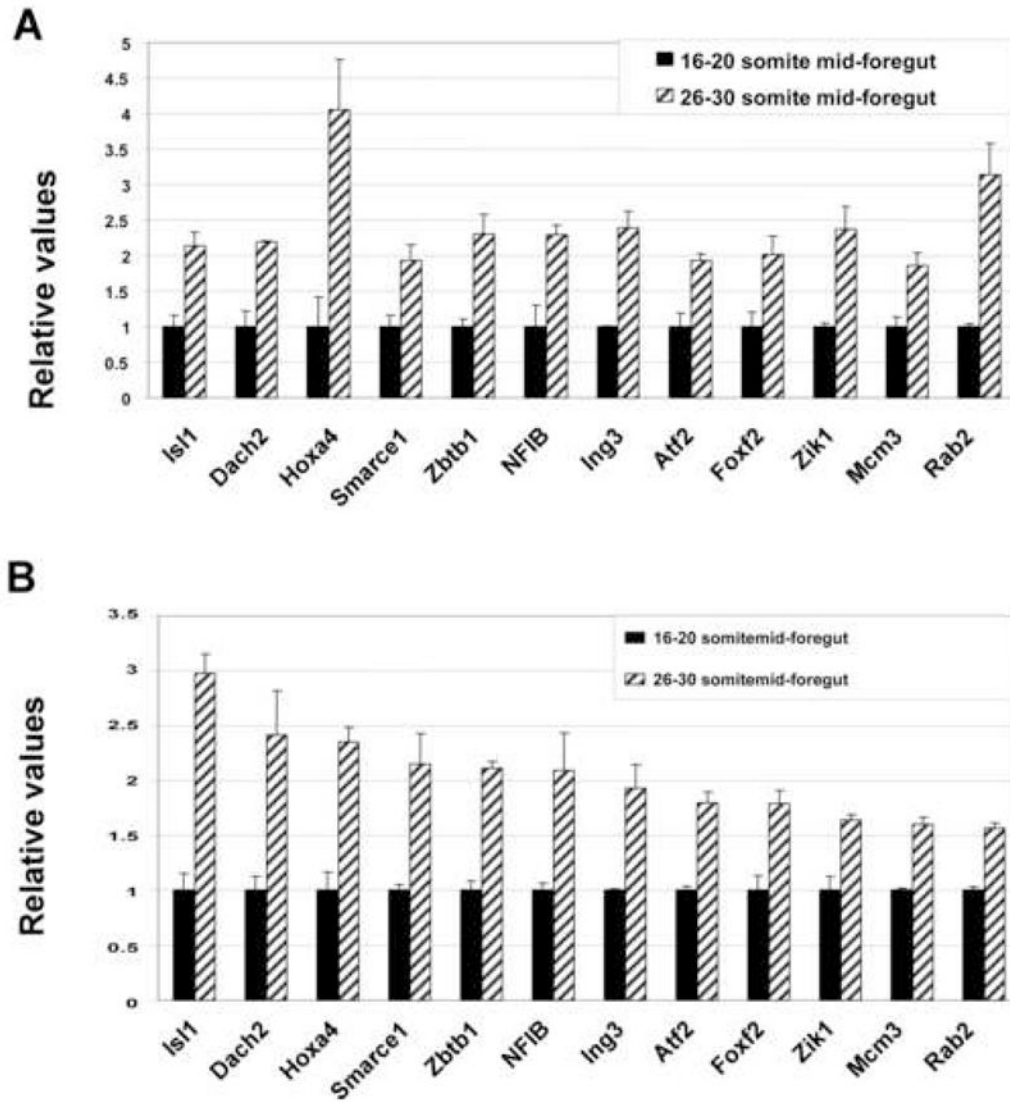


Figure 3.

Patterns of gene expression identified by K-means clustering analysis of genes that pass the ANOVA test comparing the three developmental points studied 16–20, 21–25, and 26–30 somite embryos (ANOVA $p \leq 0.05$). **A.** genes that are down-regulated from 16–20 to 26–30 somites; **B.** genes that are down-regulated from 16–20 to 21–25 somites; **C.** genes that peak at 21–25 somites; **D.** genes that are up-regulated from 16–20 to 26–30 somites; **E.** genes that are up-regulated from 21–25 to 26–30 somites. The complete list of genes is in the supplemental material. Axes: x, developmental stage; y, z-score normalized values, 0=mean of the average for each gene. ± 1 = standard deviation.

**Figure 4.**

Real time RT-PCR validation of selected transcription related genes identified by microarrays. **A.** Expression levels obtained in the microarray analysis of amplified RNA from 16–20 somite mid-foreguts (relative value =1, black bars) compared to 26–30 somite mid-foreguts (fold change relative to 16–20 somite samples, hatched bars). **B.** Real time RT-PCR validation of the genes depicted in A. Non-amplified RNA from 16–20 somite mid-foreguts (relative value =1, black bars) compared to 26–30 somite mid-foreguts (fold change relative to 16–20 somite samples, hatched bars). Data are normalized to GAPDH expression level. n=3. Error bars represent standard error of the mean.

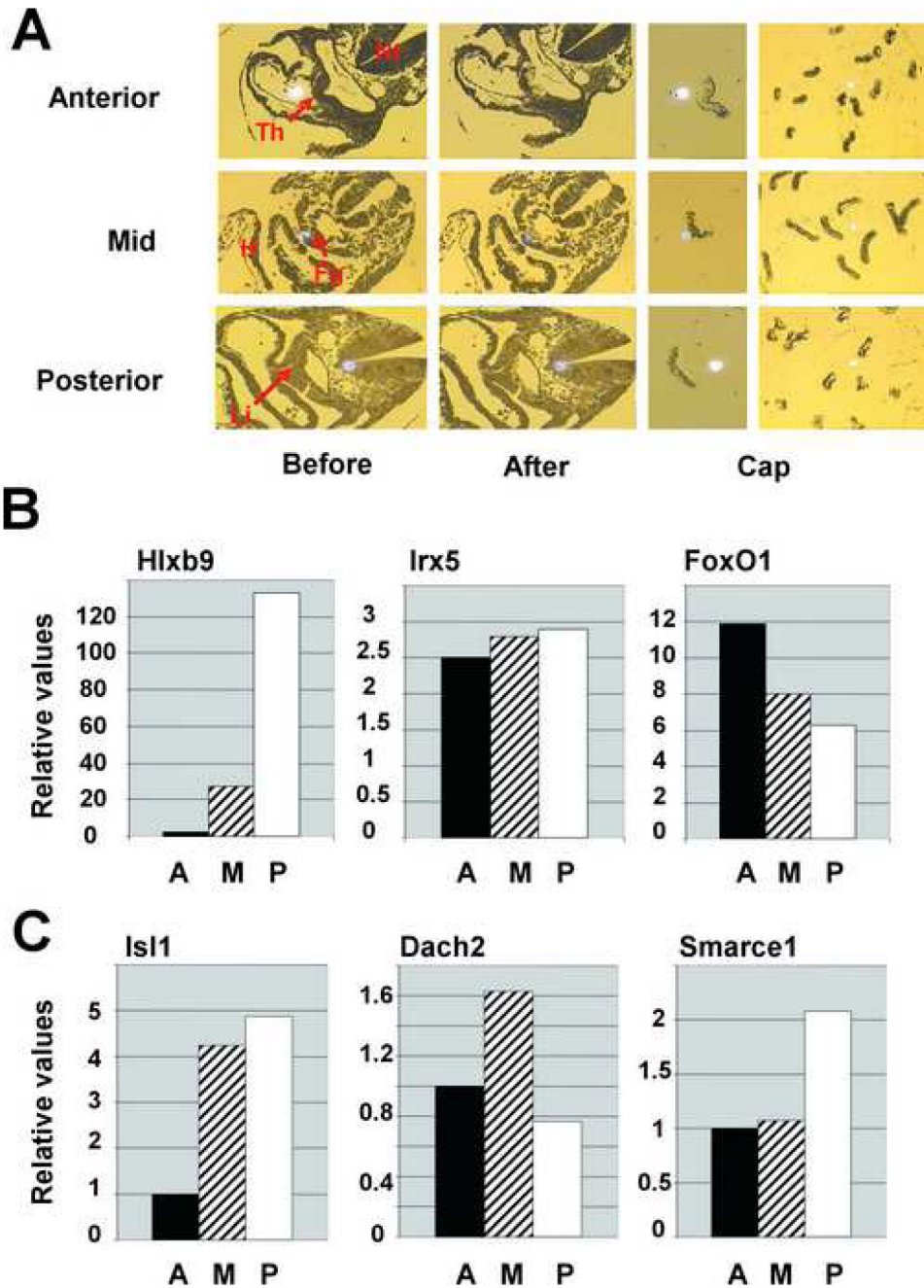


Figure 5.

A. Representative laser capture microdissection of foregut endoderm from (anterior) thyroid region, (mid) lung region, and (posterior) liver/pancreas region from embryos containing 21–25 somites. (Before) picture of a transverse tissue section before laser capture, (after) tissue remaining on the slide after dissection, (cap) tissue collected on the cap membrane. Nt, notochord; Fg, foregut; Th, thyroid bud; Li, Liver bud; H, heart. **B.** Real time RT-PCR of three selected transcription factors that show distinctive patterns of expression along anterior (A), mid (M) and posterior (P) foregut endoderm from 21–25 somite embryos. **C.** Real time RT-PCR of three selected transcription genes that show distinctive patterns of expression along anterior (A), mid (M) and posterior (P) foregut endoderm from 26–30 somite embryos.

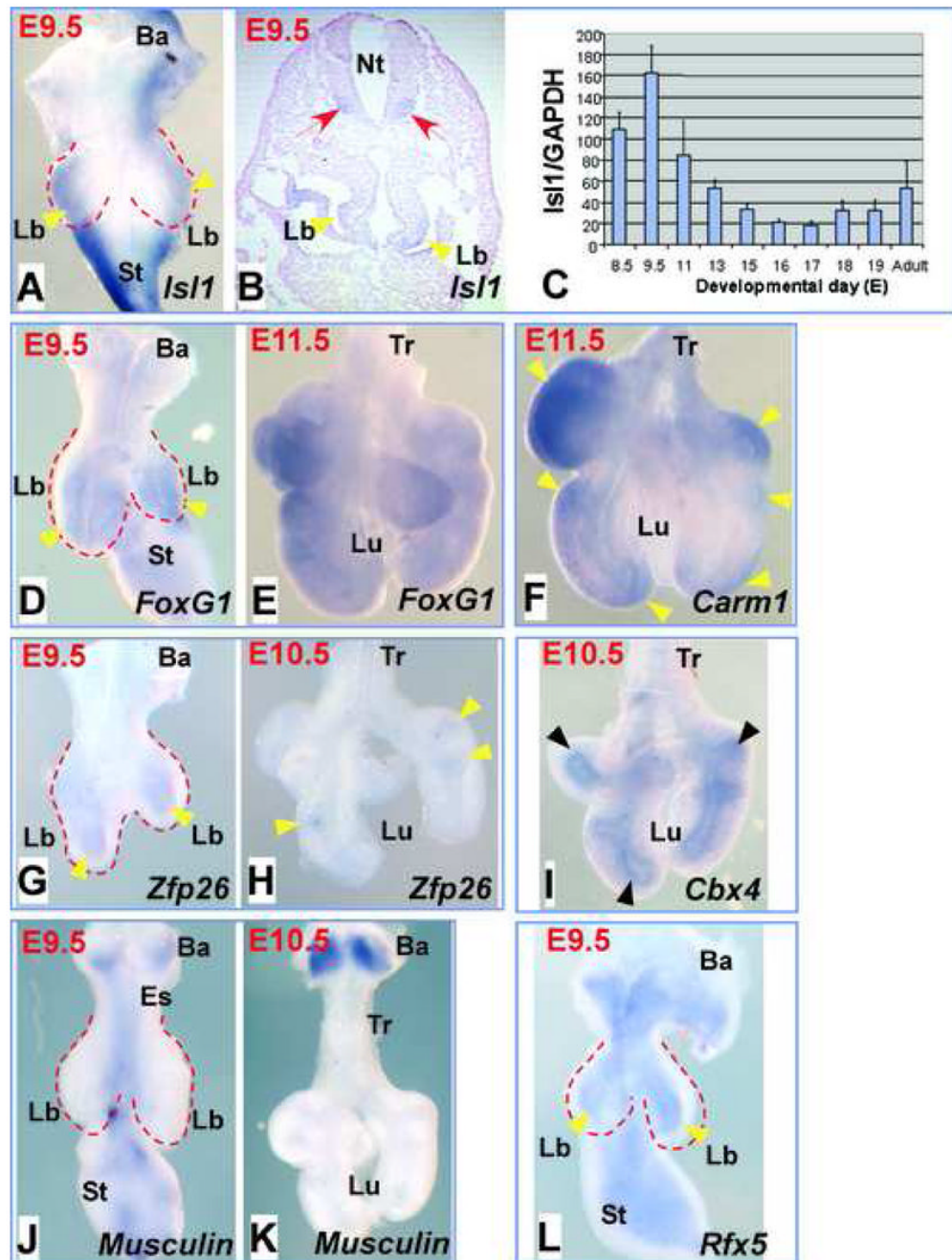


Figure 6. Pattern of expression of selected genes in the primary lung buds and developing lung determined by whole mount in situ hybridization. **A.** *Isl1* is mainly expressed in the mesenchyme of the primary lung buds (yellow arrowheads) and the stomach of embryonic foreguts at E9.5. **B.** Transverse section of paraffin embedded whole embryos after WMISH, counter stained with Fast Red, shows expression of *Isl1* in the neural tube (red arrows), the tips of the forming lung buds and the sinus venosus at E9.5 (yellow arrowheads). **C.** Expression levels of *Isl1* mRNA were determined by real time RT-PCR at different stages of lung development and in adult lung. *Isl1* expression level is normalized to GAPDH. n=3. Error bars represent standard error of the mean. **D.** *FoxG1* is expressed in the mesenchyme of the primary

lung buds (yellow arrowheads) and stomach at E9.5. **E.** FoxG1 is diffusely detected in the lung mesenchyme at E11.5 **F.** Carm1 is concentrated in the mesenchyme at the tips of the lung branches at E11.5 (yellow arrowheads). **G.** Zfp26 is expressed in the mesenchyme close to the epithelium in the forming primary buds at E9.5 (yellow arrowheads). **H.** Zfp26 is faintly detected at the tips of the branches at E10.5 (yellow arrowheads). **I.** Cbx4 is expressed in the epithelium of the lung branches at E10.5 (black arrowheads). **J.** Musculin is absent in the primary lung buds at E9.5 but is expressed in the mid foregut along the esophagus. It is also expressed in the branchial arches and stomach, likely in muscle progenitor cells. **K.** Musculin is not detected in the lung at E10.5 but expression continues in the branchial arches. **L.** Rfx5 is expressed in the subepithelial mesenchyme alongside the foregut, including the primary lung buds at E9.5 (yellow arrowheads). Fg, foregut; Nt, neural tube; H, heart, Sv, sinus venosus; Ba, branchial arches; Lb, primary lung bud; Lu, lung; Tr, trachea.

Table 1

Genes involved in transcription differentially regulated as the lung buds form.

Gene	Genes enriched at 16–20s					Genes enriched at 21–25s					Genes enriched at 26–30s				
	Affymetrix ID	Fold Change	16–20s	21–25s	26–30s	Affymetrix ID	Fold Change	16–20s	21–25s	26–30s	Affymetrix ID	Fold Change	16–20s	21–25s	26–30s
<i>Nfia</i>	1421163_a_at	-1.5	1.0	-1.5	-3.2	<i>Nfya</i>	1438245_at	1.0	4.8	2.3	<i>Bcl11a</i>	1419406_a_at	1.0	2.3	5.6
<i>Ehox</i>	1419229_at	-1.6	1.0	-2.9	-2.9	<i>Zbtb1</i>	1424750_at	1.0	2.7	2.3	<i>Six5</i>	1427560_at	1.0	4.3	4.3
<i>Sp7</i>	1418425_at	-1.1	1.0	-2.3	-2.3	<i>Afp2</i>	1426582_at	1.0	2.6	1.9	<i>Hoxa4</i>	1427354_at	1.0	1.9	4.1
<i>Twist1</i>	1418733_at	1.3	1.0	-2.0	-2.0	<i>Rfx5</i>	1423103_at	1.0	2.6	1.9	<i>Ets1</i>	1452163_at	1.0	1.9	3.1
<i>Zfp52</i>	1426471_at	-1.7	1.0	-1.9	-1.9	<i>Nr3c1</i>	1460303_at	1.0	2.6	2.4	<i>Foxp1</i>	1435222_at	1.0	1.0	3.0
<i>Fhl2</i>	1419184_a_at	-1.2	1.0	-1.9	-1.9	<i>Mafk</i>	1418616_at	1.0	2.3	1.4	<i>Msc</i>	1418417_at	1.0	1.4	2.8
<i>Hoxa1</i>	1420565_at	-1.5	1.0	-1.7	-1.7	<i>Foxm1</i>	1448833_at	1.0	1.7	1.3	<i>Hoxa5</i>	1448926_at	1.0	1.4	2.5
<i>Cebpg</i>	1451639_at	-1.6	1.0	-1.6	-1.6	<i>Meox1</i>	1417595_at	1.0	1.5	-1.4	<i>Ejfl</i>	1417540_at	1.0	2.0	2.3
<i>Rfx3</i>	1425413_at	1.0	1.0	-1.6	-1.6	<i>E2f6</i>	1448835_at	1.0	1.5	1.3	<i>Hoxb8</i>	1452493_s_at	1.0	1.5	2.3
<i>Mesp1</i>	1426557_at	1.1	1.0	-1.5	-1.5	<i>Srf</i>	1418255_s_at	1.0	1.5	1.2	<i>Zfp71-rs1</i>	1424752_x_at	1.0	1.8	2.3
<i>Evsrg</i>	1421747_at	-1.7	1.0	-1.5	-1.5	<i>Gabpb1</i>	1436232_a_at	1.0	1.5	1.2	<i>Id4</i>	1450928_at	1.0	1.7	2.2
<i>Ruvr2</i>	1425389_a_at	-1.6	1.0	-1.4	-1.4	<i>Irx5</i>	1421072_at	1.0	1.5	-1.2	<i>Isl1</i>	1450723_at	1.0	1.3	2.1
<i>Gf2h4</i>	1417093_a_at	-1.7	1.0	-1.4	-1.4	Co-factors					<i>Pitx2</i>	1424797_a_at	1.0	1.3	2.1
Co-factors						<i>Dnajc1</i>	1420500_at	1.0	3.9	2.0	<i>Sp4</i>	1437508_at	1.0	2.0	2.1
<i>Scand1</i>	1448868_at	-3.0	1.0	-2.8	-2.8	<i>Zmynd11</i>	1426531_at	1.0	2.0	1.3	<i>Foxf2</i>	1418220_at	1.0	1.9	2.0
<i>Lsm4</i>	1448622_at	-1.9	1.0	-2.7	-2.7	<i>Phr1</i>	1434937_at	1.0	1.6	-1.1	<i>Zfp37</i>	1419207_at	1.0	1.2	2.0
<i>Six1</i>	1427277_at	-1.3	1.0	-2.6	-2.6	<i>Ncor1</i>	1423200_at	1.0	1.6	1.1	<i>Rb1</i>	1417850_at	1.0	1.4	2.0
<i>Fabp1</i>	1417556_at	-2.9	1.0	-1.9	-1.9	Chromatin remodeling factors					<i>Tcf4</i>	1434148_at	1.0	1.7	1.9
<i>Hsbp1</i>	1451162_at	-1.8	1.0	-1.9	-1.9	<i>Ezh1</i>	1449023_a_at	1.0	1.8	1.4	<i>Tcfap4</i>	1418167_at	1.0	1.1	1.9
<i>Med8</i>	1431423_a_at	-1.9	1.0	-1.8	-1.8	<i>Hplbp3</i>	1415751_at	1.0	1.7	1.5	<i>Zfp26</i>	1427120_at	1.0	1.4	1.7
<i>Pdlim1</i>	1416554_at	-1.8	1.0	-1.8	-1.8	<i>Mbd2</i>	1417165_at	1.0	1.6	1.5	Co-factors				
<i>Six3</i>	1427523_at	1.1	1.0	-1.6	-1.6	<i>Ncoal</i>	1434515_at	1.0	1.5	1.4	<i>Rbbp4</i>	1454791_a_at	1.0	1.3	3.7
<i>Ptasy</i>	1418861_at	-1.3	1.0	-1.5	-1.5						<i>Zfpm2</i>	1449314_at	1.0	2.6	3.5
<i>Hengp</i>	1449295_at	-2.0	1.0	-1.5	-1.5						<i>Zfp467</i>	1419564_at	1.0	3.8	3.2
<i>Thap7</i>	1452069_a_at	-1.6	1.0	-1.4	-1.4						<i>Rab2</i>	1419946_s_at	1.0	2.4	3.1
<i>Snapec2</i>	1436703_x_at	-1.5	1.0	-1.2	-1.2						<i>Strap</i>	1419913_at	1.0	1.6	2.5
<i>Serrad3</i>	1421076_at	-1.6	1.0	-1.2	-1.2						<i>Ztk1</i>	1433946_at	1.0	1.3	2.4
Chromatin remodeling factors											<i>Iff2</i>	1417948_s_at	1.0	1.5	2.2
<i>Sap18</i>	1419444_at	-1.7	1.0	-2.2	-2.2						<i>Dach2</i>	1449823_at	1.0	1.5	2.2
<i>Hmgx3</i>	1431777_a_at	-1.4	1.0	-1.9	-1.9						<i>Khdrbs1</i>	1437389_x_at	1.0	1.9	1.9
<i>Chrac1</i>	1422505_at	-1.6	1.0	-1.6	-1.6						<i>Dr1</i>	1416018_at	1.0	1.7	1.9
<i>Ruvb1</i>	1416585_at	-1.6	1.0	-1.2	-1.2						<i>Mcm3</i>	1420029_at	1.0	1.5	1.9
<i>Sin3b</i>	1424355_a_at	-1.5	1.0	-1.1	-1.1						<i>Hmga2</i>	1422851_at	1.0	1.6	1.8
											<i>Tle1</i>	1422751_at	1.0	1.7	1.7
											<i>Ctcf</i>	1448405_a_at	1.0	1.3	1.7
											<i>Brg1</i>	1426083_a_at	1.0	1.1	1.7
											<i>Hmga2</i>	1450780_s_at	1.0	1.5	1.7
											Chromatin remodeling factors				
						<i>Suz12</i>	1449661_at	1.0	2.5	2.9	<i>Suz12</i>	1449661_at	1.0	2.5	2.9
						<i>Ing3</i>	1450760_a_at	1.0	1.6	2.4	<i>Ing3</i>	1450760_a_at	1.0	1.6	2.4
						<i>Smcy</i>	1424903_at	1.0	1.0	2.2	<i>Smcy</i>	1424903_at	1.0	1.0	2.2

Genes enriched at 16–20s			Genes enriched at 21–25s			Genes enriched at 26–30s		
Gene	Affymetrix ID	Fold Change	Gene	Affymetrix ID	Fold Change	Gene	Affymetrix ID	Fold Change
		16–20s	21–25s	16–20s	21–25s	16–20s	21–25s	26–30s
		Stat	Stat	Stat	Stat	Stat	Stat	Stat
<i>Chy4</i>	1419583_at				1.0		1.5	2.2
<i>Bmi1</i>	1448733_at			1.0	1.5		1.5	2.1
<i>Rnf2</i>	1451519_at			1.0	1.2		1.2	2.0
<i>Smarce1</i>	1422676_at			1.0	1.2		1.2	1.9
<i>Chmp1b</i>	1418817_at			1.0	1.6		1.3	1.9
<i>Carm1</i>	1419743_s_at			1.0	1.3		1.3	1.7
<i>Dnm3a</i>	1460324_at			1.0	1.3		1.3	1.7
<i>Pspc1</i>	1423192_at			1.0	1.3		1.3	1.7

Statistics (= Student's t test $p \leq 0.05$)

a= ANOVA $p \leq 0.05$

A Student's t test was used to compare the earliest vs. the latest time point (16–20 s to 26–30 s). Genes with $p \leq 0.05$ are indicated with t.

A parametric ANOVA was performed to find genes differentially expressed between two or more of the three groups. Genes with $p \leq 0.05$ are indicated with a.

Genes enriched at 16–20s are down regulated as the lung buds.

Genes enriched at 21–26s peak before lung buds.

Genes enriched at 26–30s are up-regulated as the lung buds.

Genes involved in transcription were selected and divided in three functional groups, transcription factors, co-factors, and chromatin remodeling factors.

Table 2
Selected families of transcription factors detected in the mid-foregut.

Gene	Affymetrix I	Average Signal			Gene	Affymetrix	Average Signal		
		16–20s	21–25s	26–30s			16–20s	21–25s	26–30s
Fox family									
<i>Foxal</i>	1418496_at	2093	2252	2844	<i>Gata1</i>	1449232_at	164	106	175
<i>Foxa2</i>	1422833_at	635	497	712	<i>Gata2</i>	1450333_a_	477	577	510
<i>Foxc1</i>	1419486_at	411	565	503	<i>Gata4</i>	1418863_at	288	323	330
<i>Foxd1</i>	1418876_at	355	471	460	<i>Gata5</i>	1450125_at	149	147	172
<i>Foxf2</i>	1418220_at	56	109	113 t	<i>Gata5</i>	1450126_at	452	444	448
<i>Foxg1</i>	1418357_at	193	331	394	<i>Gata6</i>	1425463_at	101	99	89
<i>Foxj2</i>	1420374_at	166	130	174	<i>Gata6</i>	1425464_at	548	580	498
<i>Foxk2</i>	1428354_at	374	857	527	Hox family				
<i>Foxm1</i>	1448833_at	374	639	473 t	<i>Hoxa1</i>	1420565_at	4171	2838	2510 a
<i>Foxn1</i>	1417748_x_	231	235	253	<i>Hoxa2</i>	1419602_at	188	256	224
<i>Foxo1</i>	1416983_s_	349	561	540	<i>Hoxa3</i>	1427433_s_	100	175	149
<i>Foxp1</i>	1421141_a_	98	81	139	<i>Hoxa4</i>	1427354_at	42	80	172 a,t
<i>Foxp1</i>	1421142_s_	218	183	301	<i>Hoxa4</i>	1420227_at	90	85	125
<i>Foxp1</i>	1421140_a_	120	205	131	<i>Hoxa5</i>	1448926_at	103	149	259 t
<i>Foxp1</i>	1435222_at	522	556	1545 a,t	<i>Hoxb1</i>	1453501_at	539	809	493
<i>Foxp1</i>	1435221_at	1733	2116	2561 a,t	<i>Hoxb2</i>	1449397_at	799	928	801
<i>Foxp3</i>	1455805_x_	341	340	363	<i>Hoxb4</i>	1460379_at	395	408	364
Tbx family									
<i>Tbx1</i>	1425779_a_	391	373	251	<i>Hoxb5</i>	1418415_at	421	512	517
<i>Tbx2</i>	1422545_at	177	232	278	<i>Hoxb7/b8</i>	1452493_s_	81	120	186 a
<i>Tbx3</i>	1448029_at	491	564	503	<i>Hoxc4</i>	1422870_at	351	620	608
<i>Tbx6</i>	1449868_at	84	100	76					
<i>Tbx20</i>	1425158_at	96	101	83					

t= Student's t-test $p \leq 0.05$

a= ANOVA $p \leq 0.05$

The table includes the average signal for genes detected in the mid-foregut and lung regions (detection $p \leq 0.05$) at 16–20s, 21–25s and 26–30s developmental stages. Only genes with a signal ≥ 100 at any stage are listed. Most genes do not change the level of expression as the lung buds. A few of them change the level of expression significantly indicated by Student's t and/or ANOVA tests.

Table 3

Selected signaling pathways detected in the mid-foregut.

Gene	Average Signal			
	16–20s	21–25s	26–30s	Average Signal
FGF pathway				
<i>FGF1</i>	1450869_at	160	169	98 t
<i>FGF7</i>	1422243_at	111	113	116
<i>FGF13</i>	1418497_at	570	664	743
<i>FGFR1I</i>	1420847_a	164	155	155
<i>FGFR3I</i>	1421841_at	375	399	441
<i>FGFRV</i>	1451912_a_	144	248	190
<i>FGFRap1</i>	1424615_at	346	321	427
Bmp pathway				
<i>Bmp1</i>	1426238_at	347	355	407
<i>Bmp4</i>	1422912_at	304	337	434
<i>Bmp7</i>	1435479_at	361	413	452
<i>BmpR1a</i>	1425491_at	248	266	296
<i>BmpR1a</i>	1425492_at	2055	3039	2974
<i>BmpR1a</i>	1425493_at	307	530	473
<i>BmpR1a</i>	1425494_s_	535	1009	780
<i>BmpR1a</i>	1451729_at	426	421	326
<i>Smad1</i>	1448208_at	815	1251	1215
<i>Smad5</i>	1451873_a_	189	279	233
<i>Grem1</i>	1425357_a_	147	125	80 a,t
<i>Bambi</i>	1423753_at	901	674	548
<i>Bmp2k</i>	1437419_at	111	169	290
Shh/Ptch pathway				
<i>Ptch</i>	<i>Ptch</i>	<i>Ptch</i>	<i>Ptch</i>	<i>Ptch</i>
<i>Smo</i>	<i>Smo</i>	<i>Smo</i>	<i>Smo</i>	<i>Smo</i>
<i>Gli1</i>	<i>Gli1</i>	<i>Gli1</i>	<i>Gli1</i>	<i>Gli1</i>
<i>Gli2</i>	<i>Gli2</i>	<i>Gli2</i>	<i>Gli2</i>	<i>Gli2</i>
<i>Hhip</i>	<i>Hhip</i>	<i>Hhip</i>	<i>Hhip</i>	<i>Hhip</i>
<i>Zic1</i>	<i>Zic1</i>	<i>Zic1</i>	<i>Zic1</i>	<i>Zic1</i>
Retinoic Acid pathway				
<i>Crabp1</i>	1448326_a_	1329	508	338
<i>Crabp2</i>	1451191_at	881	543	481 t
<i>Rai1</i>	1453200_at	255	416	315
<i>Rat12</i>	1431411_a_	1496	1135	993
<i>Sra13</i>	1433574_at	141	115	147
<i>Raet1a</i>	1420603_s_	532	300	295
Notch pathway				
<i>Notch1</i>	1418634_at	185	480	203 a
<i>Notch2</i>	1455556_at	896	876	603
<i>Notch3</i>	1421965_s_	1069	1151	1069
<i>Dll1</i>	1419204_at	179	275	252
<i>Dll3</i>	1449236_at	100	204	250 t
<i>Dx2</i>	1439429_x_	1956	1833	1867
<i>Dx3</i>	1420752_at	229	258	289
<i>Psen1</i>	1421853_at	1064	1161	1079
<i>Psen2</i>	1415679_at	2563	1924	1299 a
<i>Rbpsuh</i>	1448957_at	402	691	719
<i>Maml1</i>	1426769_s_	931	1438	1253
<i>Mib1</i>	1451818_at	278	267	235
<i>Mib2</i>	1424862_s_	135	193	202
<i>Sbno1</i>	1426559_at	334	334	143
<i>Sbno1</i>	1434612_s_	276	417	359
<i>Sbno1</i>	1451436_at	186	255	258
<i>App</i>	1420621_a_	184	212	180
<i>App</i>	1427442_a_	3160	4941	3498
<i>Aph1a</i>	1424979_at	217	216	217
<i>Aph1a</i>	1424980_s_	569	378	547
<i>Aph1a</i>	1451554_a_	238	216	192 a
<i>Fbxw7</i>	1451558_at	499	426	539
<i>Il6st</i>	1452843_at	348	521	325
<i>Nrarp</i>	1417985_at	395	527	512
<i>Trp63</i>	1418158_at	130	141	125
<i>Wdr12</i>	1448646_at	729	735	501

t= Student's t-test $p \leq 0.05$ a= ANOVA $p \leq 0.05$

The table includes the average signal for genes detected in the mid-foregut and lung regions (detection $p \leq 0.05$) at 16–20s, 21–25s and 26–30s developmental stages. Only genes with a signal ≥ 100 at any stage are listed. Most genes do not change the level of expression as the lung buds. A few of them change the level of expression significantly indicated by Student's t and/or ANOVA tests.